Medium-Voltage Modular Power Converter for Wave Energy Conversion Systems

Ahmed Darwish, Xiandong Ma, and George A. Aggidis
School of Engineering, Lancaster University.
Lancaster, UK

ABSTRACT

This paper presents and discusses the performance of a new cascaded modular power electronic converter for Wave Energy Conversion (WEC) systems. The proposed electrical power converter employs submodule units to replace the central conventional power converter aiming to bring additional benefits of scalability, lower voltage and current stresses, better efficiency, and better fault-ride-through. Because the voltages across the semiconductor switches are lower, fast devices such as Silicon Carbide (SiC) or Gallium Nitride (GaN) can be used to improve the efficiency. The proposed converter still operates at low voltage (LV) at the generator side while the outputs are connected in series to match the medium voltage (MV) grid. The paper discusses the control schemes for the power converter and presents the operational results using MATLAB/SIMULINK software.

KEY WORDS: Renewable Energy Systems (RESs); Marine Energy Systems; Wave Energy Converter (WEC); power electronic converters.

INTRODUCTION

Reducing the dependency on fossil fuel based energy sources and replacing thin with renewable energy sources (RESs) is a global economic and environmental challenge (von Jouanne and Brekeken, 2017; Tousif and Taslim, 2011; Burhanudin, Abu Hasim, Ishak, and Dardin, 2020). RESs can provide more sustainability to the energy sector as well as more security and dependency. For the European countries, the RESs will help in reaching the target of net-zero carbon emission by 2030. Examples for RESs are wind energy, solar photovoltaic, geothermal, marine, and others. The RESs technological progress will have massive economic, environmental, and social impacts and hence they are playing a major part in forming the policies which decide the governmental plans for aiding the research and industry.

In this context, Marine Energy Conversion Systems (MECSs) are considered as a promising example for RESs due to their high energy density and global availability (Darwish and Aggidis, 2022). The global annual marine energy available for extraction is estimated to be more than 100,000 TWh which is higher than the full global energy demand (IEA, 2021). Thus, understanding and improving the MECSs are essential to achieve the environmental, economical, and social goals.

MESCs harvest the kinetic or potential energy from the oceans and seas in order to convert them to electricity. This energy can be in the waves, tides, heat gradients, and currents (Halamay, Brekken, Simmons, and McArthur, 2011). The MESCs are then classified into wave energy, current, thermal and tidal energy sources. To extract the kinetic and potential energy from waves, mechanical turbines are employed to capture the energy in the waves when they are oscillating up and down. The energy is then directed to an electrical generator which will produce the required electricity (García-Medina, Özkan-Haller, and Ruggiero, 2014). The transferred thermal energy between warm water and cold water can be captured by the marine thermal energy systems. The gravitational interaction between the earth and the moon will cause tides in the oceans and seas which are in the form of kinetic energy. The mechanical turbines are employed to capture this energy and direct it to electrical generators which will be connected then to the utility grid. It is estimated by (Gunn, Stock-Williams, Quantifying, 2012) that more than 450 gigawatts of electrical power can be generated from tidal energy systems if the mechanical and electrical infrastructure exist.

Wave Energy Converters (WECs) are designed to capture the kinetic energy stored in the waves using mechanical devices and then direct it to electrical generators (Pelc and Fujita, 2011). If they are fully utilized, WECs can cover up to 60,000 TWh of the annual energy global supply according to (Grotelüschen, 2022).

The wave's energy is transferred at the wave group velocity which is normally in the range of 5 to 10 m/s (García-Medina, Özkan-Haller, and Ruggiero, 2014). The WECs can be classified according to energy capturing mechanism as Oscillating Water Column (OWC), wave activated body (WAB), and Over-topping (OT). In these types, the wave's kinetic energy is extracted using turbines and/or paddles. As shown in Fig. 1, electrical generators convert the captured kinetic and potential energy into electricity where the associated power electronic converters shape the electrical voltage and current waveforms to meet the utility grid standards. However, the back-to-back AC/DC/AC power converter has been the most common topology in the WEC systems even if it is not the optimum topology. Most of the present AC/DC/AC topologies presented for WECs are centralized systems which means that if there is a fault, the full system will be out of service until this fault is removed. Also, because the time-variant nature of the ocean's waves, the dc-link of this power converter needs large capacitors to smooth the dc-link voltage which form the main source of failure in power converters and reduce the reliability significantly.

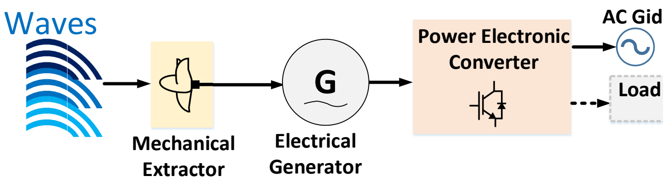

Fig.1 A brief schematic of WEC system

This paper presented a new modular power electronic converter for WECs to improve the power harvesting, controllability, power quality, and the reliability when compared with the traditional power converters. The proposed converter connects the individual WEC turbines to separate electrical generators. Then, the output electrical power are rectified and controlled by modular boost converters to generate and shape the grid/load electrical voltages and currents. The next sections will present and explain the operation of the proposed system.

CONVENTIONAL WEC POWER CONVERTER

In the WECs, the power electronic systems are designed to perform two tasks. The first task is to be integrated with the electrical generator which harvest the energy from the WEC mechanical extractor. The power converter then will convert the AC output voltages from the electrical generator into DC voltage and the energy will be stored in the DC-link capacitor. Then, the power electronic converter will convert this DC voltage, and hence current, to AC voltages and currents again but at the utility grid's frequency which is in the range of 50/60 Hz depending on the country's national grid (Darwish and Aggidis, 2022).
Although the WEC' electrical system, shown in Fig. 2, resembles other RESs such as wind systems, the output power of the WEC has a significant difference. In wind systems, the rotational speed of the mechanical extractor, which is a turbine in this case, is constant over a long time period due to the nature of the wind speeds. Moreover, the wind speed remains in one direction for a long time which means that the output voltages and currents will also have constant frequency and magnitude over this period. On the contrary, the speed of the waves are oscillatory by nature and the move up and down with a time period of 5-10 seconds. This means that the output voltages and currents of the electrical generator in this case will be oscillatory due to the positive and then negative rotational speeds. Accordingly, the WEC's power converter will behave differently to the wind turbine system's converter even if they have the same structure.
The architecture shown in Fig. 2 is the most common topology used in WEC applications where the back-to-back AC/DC/DC voltage source converter is used with a permanent magnet synchronous generator (PMSG). This is system has been originally used for wind turbine systems and has been employed in WECs according to the aforementioned similarities. The first AC/DC converter is a diode-bridge rectifier which is followed by the dc-link capacitor. The dc-link capacitor is then connected to the DC/AC inverter to generate the required sinusoidal voltages and currents. The mechanical energy extractor depends on the type of the WEC system itself. One example, as shown in Fig.2, is the rotating paddle type shown which one of the oscillating water WEC. Because it is simple to install, operate and control, the PMSG is employed. It is worth mentioning that other generator types can be used such as the doubly-fed induction generator (DFIG) which can increase the efficiency of the full system but at the expense of increasing the control complexity. Fig.3 shows examples for the generator speed versus the generator voltage for an AC/DC/AC based WEC system. The results are obtained using MATLAB/SIMULINK where the average output power is 800 W. As shown in Fig.3 (up), the generator's speed is sinusoidal due to the oscillatory nature of the waves and hence the paddle's motion. Accordingly, the waveform of the generator's output voltage is a modulated sinewave as shown in Fig.3 (down). The modulation scheme of the WEC's side AC/DC converter should modulate this waveform in order to keep the dc-link voltage in a specific range. Because this operation is complicated, the diode-bridge rectifier is employed as the AC/DC converter with leaving the dc-link to uncontrolled. Fig. 4 (up) shows the mechanical torque of the generator's shaft which is also oscillatory due to the same reason. The output power is shown in Fig.4 (down) which means that electrical power injected into the grid will be oscillatory. This will not be favorable by the utility grid as the grid code defines some strict standards regarding the power quality (Alotaibi and Darwish, 2021).

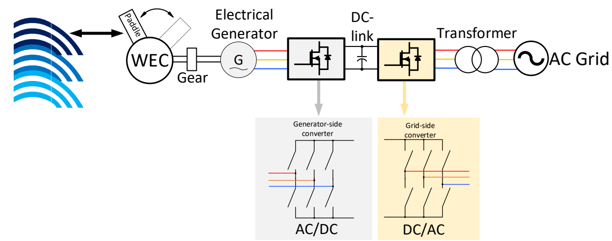

Fig.2 A conventional AC/DC/AC based WEC system.

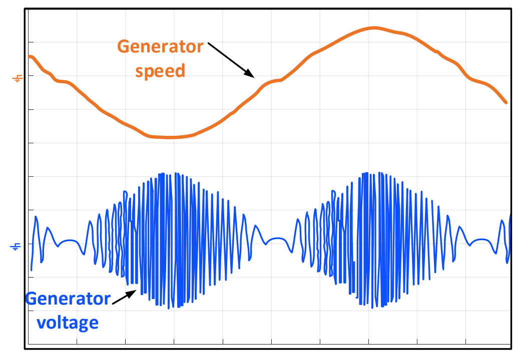

Fig. 3 MATLAB simulation results for the WEC system in Fig. 2 Generator speed: 200 r/min/div and generator no-load voltage: 20V/div – Time: 1s/div

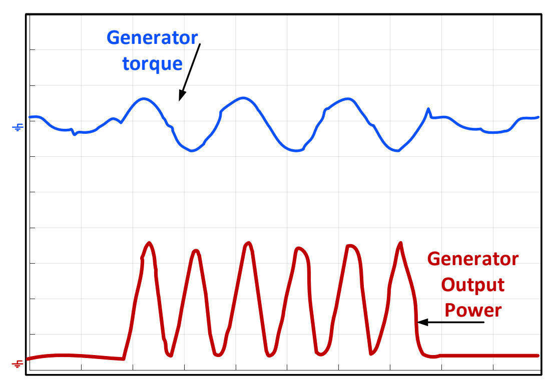

Fig. 4 MATLAB simulation results for the WEC system in Fig. 2 Generator torque: 30 Nm/ div and generator output power: 400W/div – Time: 5s/div

The AC/DC and DC/AC converter topologies employed in the WEC system in Fig. 2 are usually called in the literature as voltage source converters (VSCs). In these VSC architecture, the voltage is chopped using semiconductor devices such as insulated gate power transistors

(IGBTs), metal–oxide semiconductor field-effect transistors (MOSFETs), and diodes. Chopping the voltage at the input and output sides is simpler than chopping the current using the IGBTs and MOSFETs because they are voltage controlled devices. However, the input and output currents of the VSCs are discontinuous which necessitate for bigger filters at the input and output sides to ensure that the electrical standards are met. For example, the usual grid's standard of the total harmonic distortion (THD) in the injected current should be lower than 5% of the rms value which requires big capacitors and inductors to filter the discontinuous current from the VSC. Therefore, some researchers discussed replacing the VSC topology with current source converters (CSCs). The CSC is able to control the input and output currents of the WEC system at lower losses (higher efficiency) and lower THD in the input and output currents. The block diagram of the CSC based system is shown in Fig. 5.

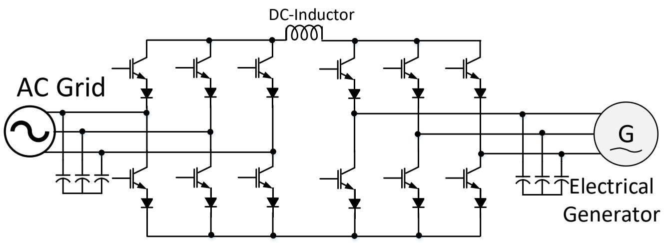

Fig. 5. CSC based WEC (McDonald, Baker, Espinoza, and Pickert, 2019)

An interesting comparison between the CSC and the VSC is carried out in (McDonald, Baker, Espinoza, and Pickert, 2019) where the authors proved that beyond certain switching frequency, the CSC topology become more efficient by reducing the power losses in the semiconductor devices. The comparison is shown in Fig. 6.

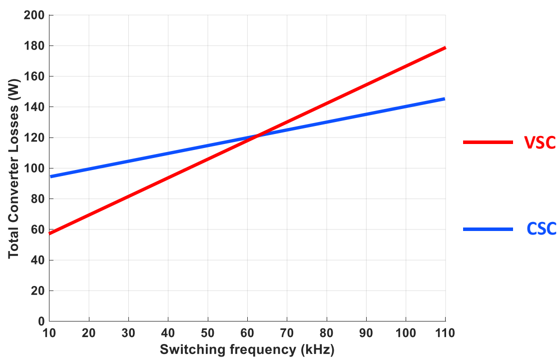

Fig. 6 Comparison between power losses in WECs based on VSC and CSC (McDonald, Baker, Espinoza, and Pickert, 2019)

However, the centralized AC/DC/AC back-to-back converters either as VSCs or CSCs means the entire WEC power is converted from the mechanical system to the grid via all semiconductor switches. This will increase the power losses and the probability of full shutdown if one of these devices fails. Although the connection to the medium-voltage (MV) grids is possible using transformers, the back-to-back converter has a limited capabilities to boost the voltage from the generator side to meet the MV grid voltage level. Therefore, Modular Multilevel Converters (MMCs) have been introduced to solve this problem in other RESs such as wind and solar PV systems. The next section will present a proposed modular converter suitable for WEC applications which can improve the performance by providing modularity, scalability, and voltage boosting capabilities.

THE PROPOSED MODULAR CONVERTER

Fig. 7 shows the proposed modular boost converter (MBC) for the WEC systems. The MBC is formed of series connected power units (PUs) which are responsible for harvesting the wave energy. The turbine in each PU is coupled with a PMSG generator to convert the kinetic wave energy into electrical energy. The output power of the generator is directed to a full bridge rectifier with a dc-link capacitor. The dc-link capacitor is then connected to a submodule (SM) operating as a boost converter to generate a variable voltage. The variable voltages of the series connected PUs will be summed together to form the total output voltage of the MBC. The next subsections will explain the operation of the proposed converter in both SM and overall levels.

SM operation

As shown in Fig. 7, the boost converter is used as the basic SM of the modular converter. Although this boost converter can generate output voltage v higher than the input dc-link voltage v_{dc}, this output voltage will be always of the same polarity. Therefore, each two successive SMs will be connected in series but in opposite polarity as shown in Fig. 7. Assuming that the converter is formed of n PUs and SMs, the first two successive SMs in phase a will generate output voltages as follows:

$$v_{1a+} = V_1 \sin(\omega t + \theta) + V_{dc1} \tag{1}$$

$$v_{1a-} = V_1' \sin(\omega t + \pi + \theta) + V_{dc1}' \tag{2}$$

Because the two SMs are connected in series but with opposite voltage polarities, their total voltage is:

$$v_{1a} = V_1 \sin(\omega t + \theta) + V_{dc1} - V_1' \sin(\omega t + \pi + \theta) - V_{dc1}' \tag{3}$$

If the voltage magnitudes are equal as $V_1 = V_1' = V$ and $V_{dc1} = V_{dc1}' = V_{dc}$, the total voltage of the two SMs is:

$$v_{1a} = 2V \sin(\omega t + \theta) \tag{4}$$

The output voltage in Eq.4 is pure sinusoidal and hence all SMs can be connected in series to match the grid voltage. Because the system will be connected to the three-phase AC grid, the operation will be the same for the other two phases b and c but with the -120º and +120º phase shifts in the angle.

For the boost converter, it is well known that the relation between the input and output voltages is obtained from the duty-cycle ratio δ as follows:

$$v = \frac{1}{1-\delta} v_{dc} \tag{5}$$

Therefore, the duty-cycle ratios for the two successive SMs in phase a can be concluded from the input and output voltages as:

$$\delta_{1a+} = \frac{v_{1a+} - v_{dc}}{v_{1a+}} \qquad \delta_{1a-} = \frac{v_{1a-} - v_{dc}}{v_{1a-}} \tag{6}$$

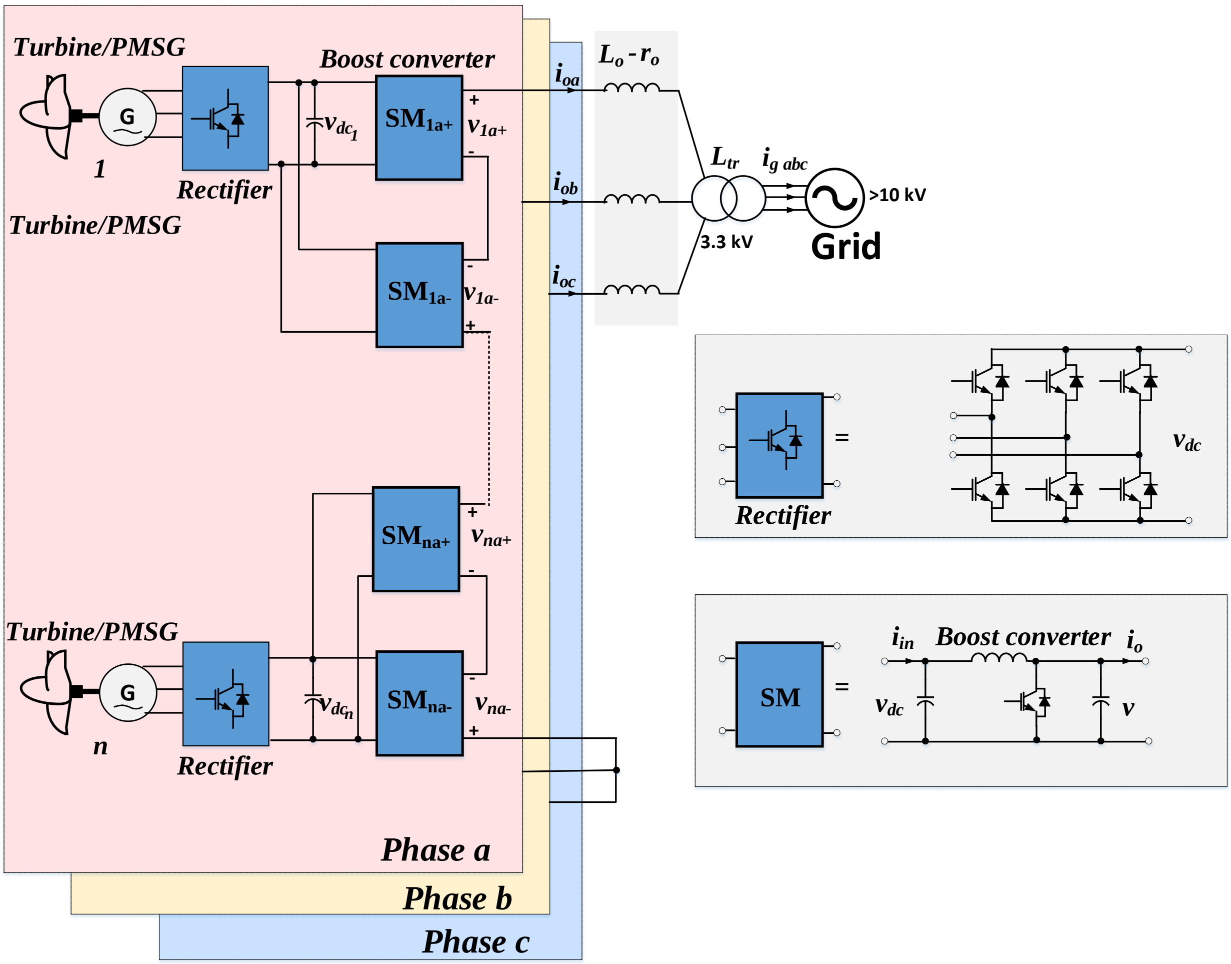

Fig. 7. The proposed MBC converter for WEC applications

Three-phase overall operation

The output terminals of the proposed MBC are connected to the grid via a step-up transformer as shown in Fig. 7. The MBC terminal three-phase voltage can be expressed as:

$$v_{ta} = V_t \sin(\omega t + \theta) \tag{7}$$

$$v_{tb} = V_t \sin(\omega t + \theta - 120^\circ) \tag{8}$$

$$v_{tc} = V_t \sin(\omega t + \theta + 120^\circ) \tag{9}$$

To give an example, the relation between the terminal voltages of phase *a* and the output voltages of the SMs can be obtained from:

$$v_{ta}(t) = \sum_{i=1}^{n} v_{ia}(t) \tag{10}$$

If the MBC converter is operating as a unity power factor, the three-phase output currents are expressed as:

$$i_{oa} = I_o \sin(\omega t) \tag{11}$$

$$i_{ob} = I_o \sin(\omega t - 120^\circ) \tag{12}$$

$$i_{oc} = I_o \sin(\omega t + 120^\circ) \tag{13}$$

These currents will determine the MBC's active power P to be injected into the MV grid. Assuming that L_t and r_t are the total inductance and resistance of the output filter and transformer as referred to the MBC at the primary side, the magnitude of the output current I_o as well as the magnitude and the angle of the terminal voltage V_t and θ can be calculated from:

$$I_o = \frac{2NP}{3V_g} \tag{14}$$

$$\theta = \tan^{-1}\left[\frac{\omega L_t I_o}{V_g / N + r_t I_o}\right] \tag{15}$$

$$V_t = \left[\frac{V_g / N + r_t I_o}{\cos(\theta)}\right] \tag{16}$$

where V_g is the magnitude of the grid's voltage and N is the transformer turn's ratio.

The mathematical analysis in this subsection will enable the MBC to inject the active power P into the grid as long as the three-phase grid voltage is measured and the circuit parameters such as L_t, r_t, and N are all known, constant and balanced. However, a control system is required to operate the system in case of unbalance and/or parameters' variation.

CONTROL SYSTEM

The control system of the proposed MBC in this paper is split into two levels. The first is the SM-level controller where each SM is controlled individually based on the average power delivered by the mechanical turbine and the coupled electrical generator. The second is the system-level controller which adjusts the full voltage of the MBC in order to generate the required output current and inject it into the grid. The following subsections will explain the two levels.

SM controller

In this level, the dc-link voltage of the SM is controlled based on the available mechanical power from the waves. Accordingly, a PU with higher power will have higher dc-link voltage by the same power ratio when compared with the other PUs. This is controlled by the machine side controller as shown in Fig. 8. The reference dc-link voltage is subtracted from the actual one and the voltage error is controlled by the proportional-integral (PI) controller using the rectifier modulation index M_r. Then, the grid-side controller will control the output voltage of the SM based on the power ratio and hence the dc-link voltage ratio. The grid-side controller is controlled by the duty-cycle ratios as explained in Eqs. 4~7 but with a proportional-resonant (PR) controller because the output voltage is sinusoidal.

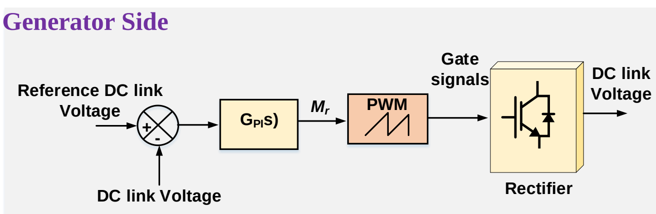

(a) Generator side Controller

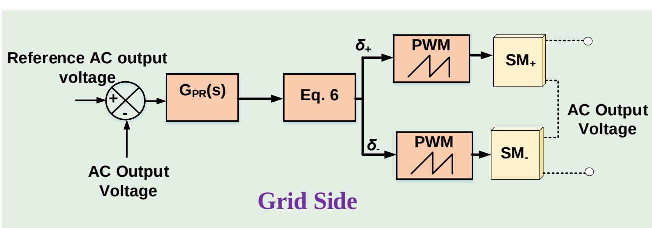

(b) Grid side controller

Fig. 8 SM-level controllers.

The PI and PR controllers transfer functions are expressed as:

$$G_{PI}(s) = k_p + \frac{k_r}{s} \qquad (14)$$

$$G_{PR}(s) = k_p + \frac{k_r s}{s^2 + \omega^2} \qquad (15)$$

where k_p, k_i and k_r are the control gains while ω is the grid's angular frequency. The tuning of these controllers are not in the scope of this paper and will be discussed in further publications.

System-level controller

This controller generates the full output voltage of the MBC and controls the output current and hence current. As shown in Fig. 9, the total available power is calculated by summing the individual PUs powers and accordingly the reference grid current is calculated. To increase the system's stability, an additional loop can be inserted in the system-level controller presented in Fig. 9 to improve the dynamic response of the voltage and hence the grid current. The values of the grid current and the associated output current from the MBC are calculated based on Eqs. 14~16. Because the output current is sinusoidal, the PR controller will be used in this case to generate the overall duty cycle ratios of the three phases which will be sent to all SMs and added with the individual duty cycle ratio δ_{SM}. Finally, the duty-cycle ratios from the system-level controller will be added with the corresponding duty-cycle ratios from the SM-level controllers to operate the associated boost converters in the SMs.

MBC SIMULATION RESULTS

MATLAB/SIMULINK software will be used in this section to show the operation of the proposed MBC. The operation of the converter will be presented in two different case studies. In the first one, the output power of the PUs will be considered constant and hence all SMs will generate the same powers. The dc-link voltage of all capacitors in the different SMs will be almost equal and the output electrical power will be shared evenly by the different SMs. In the second scenario, the output power of the PUs will change at the middle of the simulation time to show the capability of the control systems to continue operation during this disturbance. The electrical generators will be chosen as PMSGs while the conventional voltage source rectifier (VSR) will be selected for the AC/DC stage. The system parameters are listed in Table 1.

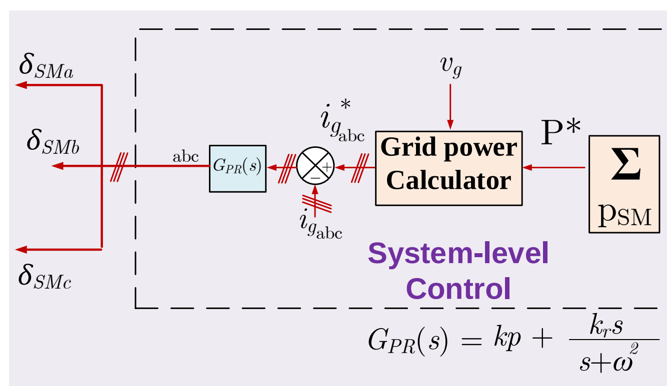

Fig. 9 System-level controller

Table 1. Parameters of the SIMULINK/MATLAB

Parameter	Value
Wave period	5 s
Electrical Generator	Three-phase PMSM
Number of PUs per phase	n = 8
SM rated power	p_{SM} = 1.5 kW
RMS grid voltage	12.25 kV (line-to-line)
Transformer's turns ratio	3.71
Grid frequency	50 Hz
Boost converter's switching frequency	f_s = 50 kHz
Grid impedance (referred to primary)	r_t = 0.5 Ω and L_t = 5 mH

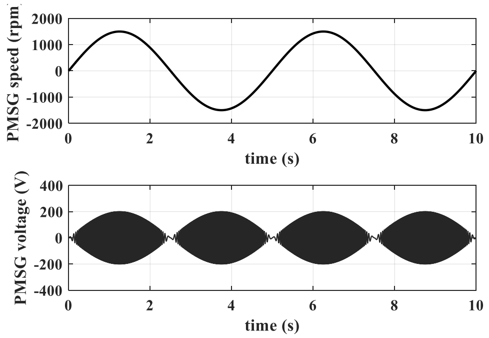

(a) PMSG speed (above) and phase a voltage (below)

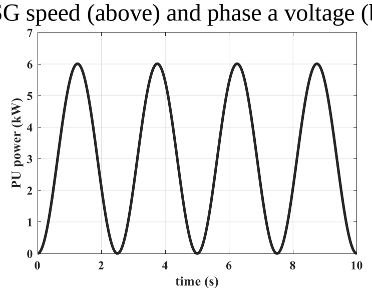

(b) PU output power

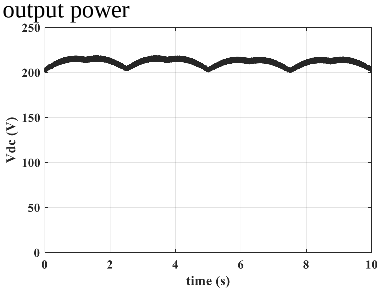

(c) DC-link voltage

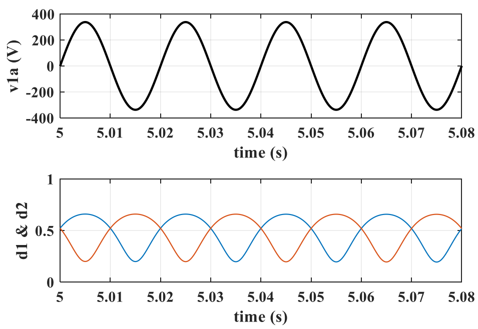

(d) Two successive SMs voltage (above) and SMs duty-cycle ratio (below)

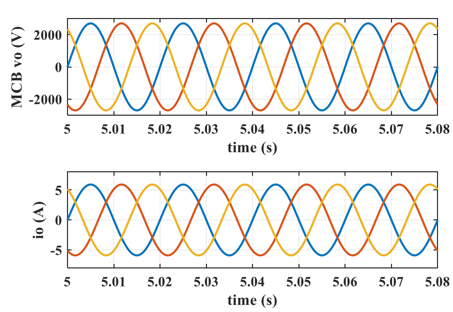

(e) MBC converter output voltage (above) and current (below)

Fig. 10 Simulation results for the MBC during equal power generation from the WEC turbines.

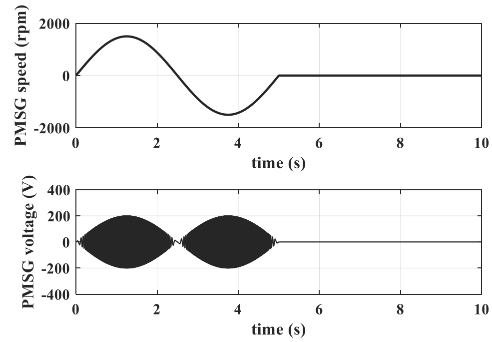

(a) Fault PU PMSG speed (above) and phase a voltage (below)

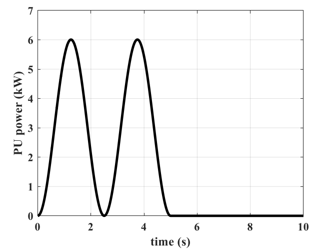

(b) Faulty PU output power

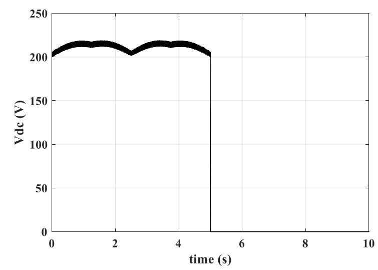

(c) DC-link voltage

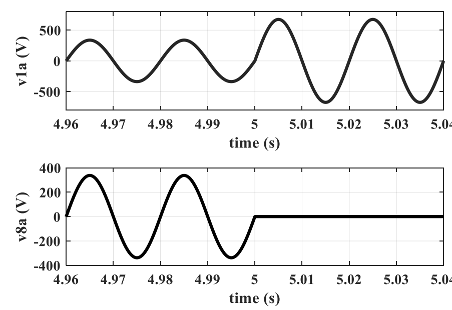

(d) Two successive SMs voltage of the healthy PU (above) and of the faulty PU (below)

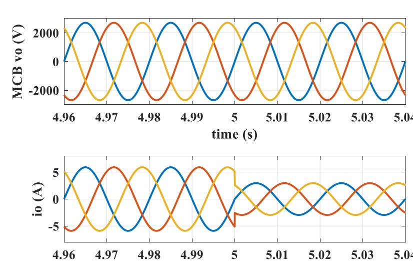

(e) MBC converter output voltage (above) and current (below)

Fig. 11 Simulation results for the MBC during faulty power generation from the WEC turbines.

MBC operation with equal PUs generation

Fig. 10 shows the operation of the proposed MBC in the normal conditions when all PUs are generating equal power. The assumed wave speed will lead to the PMSG speed as shown in Fig. 10a with the associated output voltage of phase *a*. Fig. 10b shows the output power for the first PU while the other seven are identical. Fig. 10c show the dc-link voltage which is controlled by the VSR using the control system mentioned earlier in Fig. 8. Fig. 10d sows the output voltage of the first two successive SMs in phase a. The voltages of the other SMs are identical at the same frequency and magnitude. The duty-cycle ratios of the two SMs are shown also in Fig. 10d to ensure that they are in the acceptable range for boost converters which is normally kept below 0.75. Finally, Fig. 10 e shows the output voltages and currents from the proposed MBC when seen from the primary side of the step-up transformer.

MBC operation with faulty units

Fig. 11 shows the operation of the MBC when the bottom half of the PUs are out of service due to an unplanned fault. This fault is assumed to start at t = 5s. Fig. 11a shows the PMSG speed and voltage for one of the faulty units while Fig. 11b shows the associated output power of this unit. Fig. 11c shows the dc-link voltage of the faulty unit when it stopped generating power at the fault moment. Fig. 11d shows the output voltages of the healthy PU's SMs (above) with the same voltages in the faulty unit (below) where the faulty units had to increase the generated power to compensate the reduction caused by the faulty units. Finally, Fig. 11e shows the output voltages and currents. It can be seen that the output current is reduced by 50% because half of the PUs are out of service.

CONCLUSIONS

The paper proposed a new modular converter based on the conventional boost converter for WEC applications. The proposed MBC converter is capable of harvesting and collecting the generated power from the WEC units, shaping the associated voltages and current, and control the total injected power to the MV grid through a step-up transformer. If the number of the WEC turbines and PUs are increased, the generated voltage can be increased significantly and hence the MBC may not need the step-up transformer. The mathematical analyses and simulation results have shown the capability of the MBC to keep operation during the faulty conditions when some of the WEC turbines are out of service or some of the power electronic SMs fail. The paper also presented the control algorithms to operate the MBC based on PI and PR controllers.

REFERENCES

von Jouanne, A.; Brekken, T.K.A. "Ocean and Geothermal Energy Systems". *Proc. IEEE* 2017, 105, 2147–2165

Tousif, S.M.R., Taslim, S.M.B (2011) "Producing electricity from geothermal energy," *In Proceedings of the 2011 10th International Conference on Environment and Electrical Engineering*, Rome, Italy, 8–11 May 2011; pp. 1–4.

Burhanudin, J., Abu Hasim, A.S.; Ishak, A.M.; Dardin, S.S (2022). "A Review of Power Electronics for Nearshore Wave Energy Converter Applications," *IEEE Access*, 10, 16670–16680

Darwish, A., Aggidis, G.A (2022). "A Review on Power Electronic Topologies and Control for Wave Energy Converters," *Energies 2022*, 15, 9174. https://doi.org/10.3390/en15239174

IEA. "Key World Energy statistics (2021)" *Available online*: https://iea.blob.core.windows.net/assets/52f66a88-0b63-4ad2-94a5-29d36e864b82/KeyWorldEnergyStatistics2021.pdf

Halamay, D.A.; Brekken, T.K.A., Simmons, A, and McArthur, S (2011). "Reserve requirement impacts of large-scale integration of wind, solar, and ocean wave power generation," *IEEE Trans. Sustain. Energy* 2, 321–328.

García-Medina, G, Özkan-Haller, H.T, and Ruggiero, P (2014) "Wave resource assessment in Oregon and southwest Washington, USA," *Renew. Energy*, 64, 203–214.

Pelc, R, and Fujita, R.M (2022) "Renewable energy from the ocean," *Mar. Policy*, 26, 471–479

Grotelüschen, F (2022) "Scientists Race to Develop Floating Wind Farms," *Deutsche Welle*. Available online: http://www.dw.de/scientists-race-to-develop-floating-wind-farms/a-16540081 (accessed on 16 October 2022).

McDonald, S. P., Baker, N. J., Espinoza, M., and Pickert, V (2019) "Power-takeoff topology comparison for a wave energy converter,'" *Journal of Engineering*, vol. 2019, no. 18, pp. 5012-5017

Alotaibi, S, Darwish, A (2021) "Modular Multilevel Converters for Large-Scale Grid-Connected Photovoltaic Systems: A Review,'" *Energies*, vol. 14, no. 19 pp. 6213-6243